



Star-formation in the Coalsack Loop

V. Golev¹ and N. Kaltcheva²

¹ Department of Astronomy, Faculty of Physics, St Kliment Ohridski University of Sofia, 5 James Bourchier Blvd., BG-1164 Sofia, Bulgaria, e-mail: valgol@phys.uni-sofia.bg

² Department of Physics and Astronomy, University of Wisconsin Oshkosh, 800 Algoma Blvd., Oshkosh, WI 54901, USA, e-mail: kaltchev@uwosh.edu

Abstract. The giant Galactic H II region known as the Coalsack Loop, which is associated with the H I supershell GSH 305+01–24, provides a unique opportunity to study the OB-star influence on the surrounding interstellar material. The bright OB-stars within this region contribute a sufficient wind injection energy consistent with the observed size and expansion velocity of the supershell. The derived age distribution of the OB-stars is suggestive for a continuous star-formation where the youngest stars are located at the supershell's periphery.

Key words. Stars: early type – open clusters and associations: individual: Centaurus star-forming field – ISM: individual objects: GSH 305+01–24

1. Introduction

The most prominent sites of massive star-formation in the Milky Way are usually associated with supershells in star-forming complexes along the spiral arms. The Centaurus star-forming field represents part of the Carina-Sagittarius arm in both the two-armed and four-armed models of the Galaxy (Humphreys & Kerr 1974). The field is dominated by the H I supershell GSH 305+01–24 (McClure-Griffiths et al. 2001) and its optical counterpart, the Coalsack Loop (Walker & Zealey 1998).

In this contribution, several multi-wavelength surveys (Wisconsin H α Mapper Northern Sky Survey, Southern H α Sky Survey Atlas, MSX Mid-IR Galactic Plane Survey, WISE All-Sky Data Release, CO survey of the Milky Way, and the Southern Galactic Plane H I Survey) are combined with available intermediate-band *uvby* β photometry

(Hauck & Mermilliod 1998) and polarization measurements (Heiles 2000) in order to study the spatial correlation between the OB-stars and the neutral and ionized material in the GSH 305+01–24 supershell and the energetics of their interaction.

2. Massive stellar content of GSH 305+01–24

The massive stellar content of the H I supershell GSH 305+01–24 is reliably identified by the means of *uvby* β photometry which, for this field, is 85 – 90% complete in the 11.5–12 magnitude range for O–B9 spectral types (Kaltcheva et al. 2013). We redefine the Cen OB1 association, selecting photometrically 133 stars at an average distance 1.8 ± 0.4 kpc located inside GSH 305+01–24. An estimate of the individual ages of these stars via the evolutionary tracks and isochrones by

Ekström et al. (2012)¹ results in \log age of 7.09 ± 0.18 (~ 12.3 Myr) for the average age of the association. In addition, we provide estimates of the distance and age of the young open cluster NGC 4755 (1.97 kpc, ~ 15.1 Myr, respectively), also located inside the shell. The HR-diagram for the redefined Cen OB1 association and NGC 4755 is shown in Fig. 1. The distribution of stellar age across the shell indicates that star-formation started in this region about 15 Myr ago with NGC 4755 and progressively propagated toward the walls of the shell (see for details Kaltcheva et al. (2013), and the case study of NGC 602 by Carlson et al. (2007)). In Fig. 2 a high-resolution near-IR $7^\circ \times 2^\circ$ equatorial strip over the GSH 305+01-24 shell is shown, based on observations with Spitzer Space Telescope, publicly available at <http://irsa.ipac.caltech.edu/data/SPITZER/>. The image is dominated by G305.4+0.1 H II complex, a major star-formation region associated with several H II regions, for details see e.g. Clark & Porter (2004). The stars of the redefined association are shown with circles proportional to the star's age.

The cumulative effect of the stellar winds of the selected stars and NGC 4755 is sufficient to produce the observed size of the H I shell. This conclusion is supported by the total kinetic energy deposit into the surrounding ISM supplied by massive stars during their lifetime estimated for each star by stellar models. Our results, based on revised stellar content and distance to GSH 305+01-24, are in agreement with the conclusions of McClure-Griffiths et al. (2001) and the models of Silich, Elias & Franco (2008) that the GSH 305+01-24 is a wind-blown shell.

The GSH 305+01-24 supershell is located in the direction of the Lower Centaurus-Crux association, which is likely to be our closest giant star-forming complex (Comerón 2001; Elias et al. 2009)). The available *uvby* β data allows us to identify a foreground layer of very young stars at 1 kpc and to investigate its connection to both GSH 305+01-24 and the foreground GSH 304-00-12 H I shells.

¹ <http://obswww.unige.ch/Recherche/evoldb/index/>

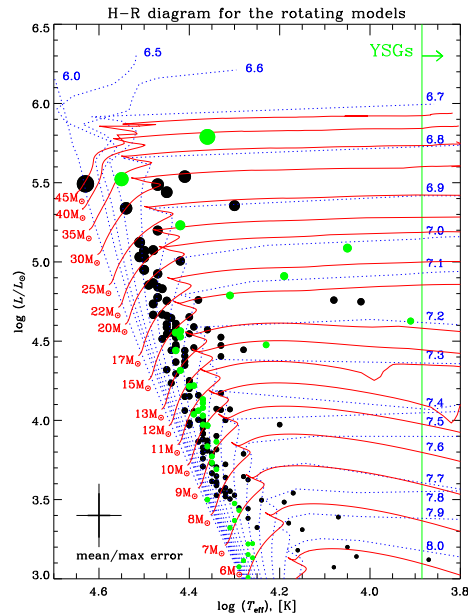


Fig. 1. The HR-diagram for the redefined Cen OB1 association (black symbols) and NGC 4755 (green symbols). The evolutionary tracks and isochrones from Ekström et al. (2012) utilized via the Geneva stellar models interactive tools are shown. Models with initial metallicity 0.014 (solar) and initial rotation rate 0.40 are used. The size of the symbols corresponds to the mass of the stars.

3. Polarization of starlight toward GSH 305 + 01 - 24

Optical polarimetry of bright stars is useful to study the large-scale properties of the magnetic field in H II regions or H I supershells. Mapping the magnetic field orientation toward the disk of the Milky Way could contribute to our understanding of the large-scale star-forming processes. Polarization measurements for a significant number of OB-stars is available toward this supershell. Since the observed star-light polarization at optical wavelengths is caused by selective absorption by magnetically aligned interstellar dust grain along the line of sight (see Fosalba et al. (2002) and references therein for details), the available data contains information about the large-scale component of the Galactic magnetic field.

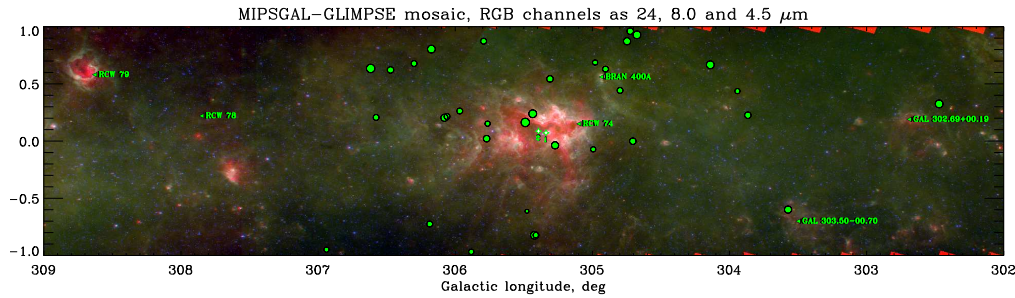


Fig. 2. High-resolution near-IR $7^\circ \times 2^\circ$ equatorial strip over the GSH 305+01-24 shell. The association stars are shown with green circles proportional to the age of the stars. Some of the known nebulae are shown too. The central clusters Danks 1 and Danks 2 of G305 complex are shown with symbols marked as '1' and '2'.

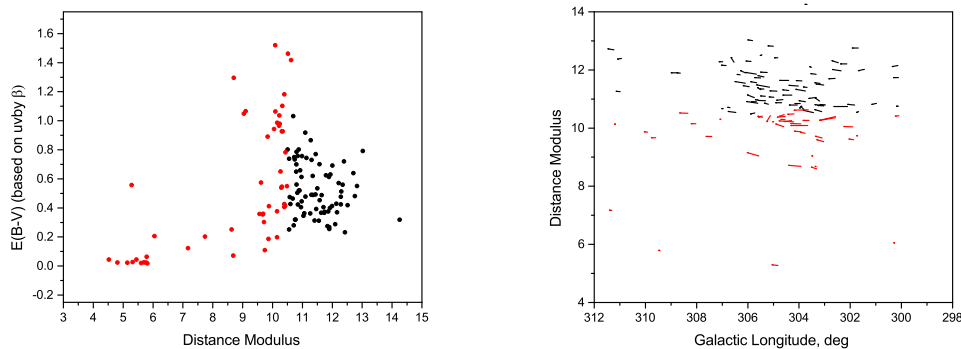


Fig. 3. Diagrams $E(B-V)$ vs. true Distance Modulus and true Distance Modulus vs. Galactic Longitude for the stars toward Centaurus with optical polarization measurements and $uvby\beta$ data.

It is particularly useful when polarization is combined with reliable distance and color excess estimations. The stars toward Centaurus with available optical polarization measurements and $uvby\beta$ data are shown in Fig. 3. The massive population of GSH 305+01-24 and the foreground young stars closer than 1 kpc are presented with different colors. The steep increase in the color excess at 1 kpc is due to stars seen toward the G305 H II complex (G305.4+0.1). Optical polarization vectors are plotted in Fig. 4 where the $H\alpha$ data are taken from Finkbeiner (2003). In comparison to the adjacent large-scale star-forming fields in the 4th Galactic quadrant, the polarization vectors are parallel to the disk, showing just small de-

viations. The vectors associated with the stars in the shell show, however, twice less deviation in their polarization angles in comparison to the vectors associated with the foreground young stars.

Acknowledgements. This work is supported by the National Science Foundation grant AST-0708950. N.K. acknowledges support from the SNC Endowed Professorship of International Relations at the University of Wisconsin Oshkosh. We acknowledge the use of SIMBAD database, operated at CDS, Strasbourg, France, and NASA's SkyView Virtual Observatory (<http://skyview.gsfc.nasa.gov>), a service of the Astrophysics Science Division at NASA/GSFC and the High Energy Astrophysics Division of the SAO.

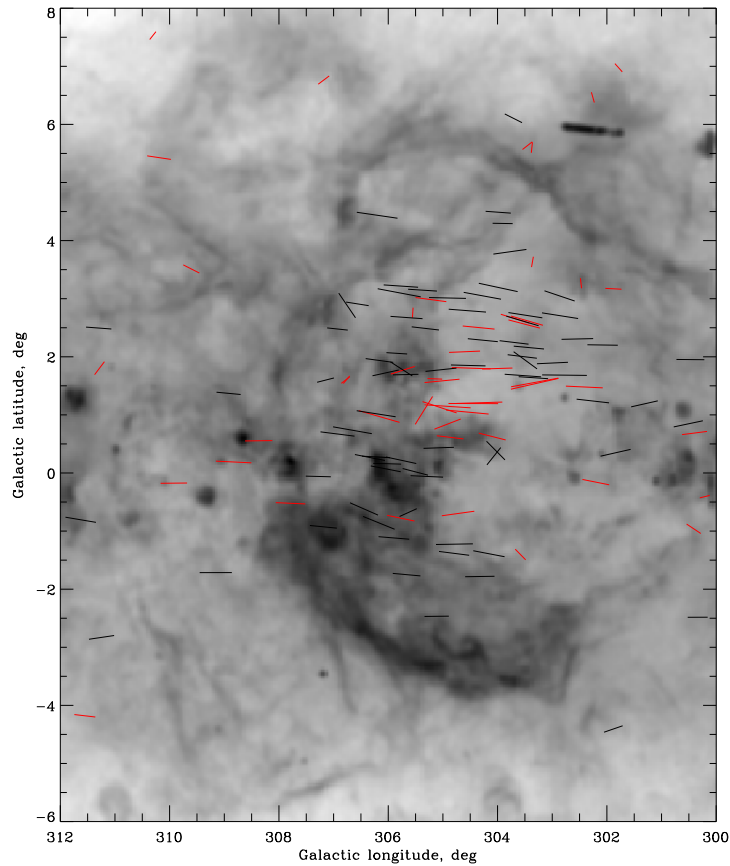


Fig. 4. Optical polarization measurements plotted on an $H\alpha$ image of the Coalsack Loop for the stars included in Fig. 3. The length of each line is proportional to the percentage linear polarization and the angle is θ_{gal} .

References

- Carlson, L. R., Sabbi, E., Sirianni, M., et al. 2007, *ApJ*, 665, L109
 Clark, J. S., Porter, J. M. 2004, *A&A*, 427, 839
 Comerón, F. 2001, *A&A*, 365, 417
 Humphreys, R. M. & Kerr, F. J. 1974, *ApJ*, 194, 301
 McClure-Griffiths, N. M., Dickey, J. M., Gaensler, B. & Green, A. J. 2001, *ApJ*, 562, 424
 Walker, A., Zealey, W. J. 1998, *PASA*, 15, 79
 Hauck, B. & Mermilliod M. 1998, *A&AS*, 129, 431
 Heiles C. 2000, *AJ*, 119, 923
 Kaltcheva, N., Golev, V., Moran, K. 2013, *A&A*, in press
 Ekström, S., Georgy C., Eggenberger P. et al. 2012, *A&A*, 537, A146
 Silich, S., Elias, F., Franco, J. 2008, *ApJ* 681, 1327
 Elias, F., Alfaro, E. J., Cabrera-Caño, J. 2009, *MNRAS*, 397, 2
 Fosalba, P., Lazarian, A., Prunet, S., Tauber, J. A. 2002, *ApJ*, 564, 762
 Finkbeiner, D. P. 2003, *ApJS*, 146, 407